Silica-Based Iminodiacetic Acid Functionalized Adsorbent for Ni Hydrometallurgical Extraction of Nickeliferous Laterite

Xin Li
Engineering and Technology Research Center for Inorgnic Type Ion-Exchange Resin, Henan University, Kaifeng 475004, People's Republic China

School of the Chemistry and Environment, Jiaying University, Meizhou 514015, People's Republic China

Baohua Li
Engineering and Technology Research Center for Inorgnic Type Ion-Exchange Resin, Henan University, Kaifeng 475004, People's Republic China

Shan Wu
Engineering and Technology Research Center for Inorgnic Type Ion-Exchange Resin, Henan University, Kaifeng 475004, People's Republic China

School of the Chemistry and Environment, Jiaying University, Meizhou 514015, People's Republic China

Jingbing Li and Qitai Xu
Engineering and Technology Research Center for Inorgnic Type Ion-Exchange Resin, Henan University, Kaifeng 475004, People's Republic China

Zhiqiang Yang, Yuqiang Liu and Shaohua Wang
Jinchuan Group Limited, Jinchang 737100, People's Republic China

Dongsheng Chen
Engineering and Technology Research Center for Inorgnic Type Ion-Exchange Resin, Henan University, Kaifeng 475004, People's Republic China

DOI 10.1002/aic.13774
Published online March 2, 2012 in Wiley Online Library (wileyonlinelibrary.com).

A novel silica-based iminodiacetic acid functionalized adsorbent was fabricated and then used to nickel hydrometallurgical extraction for low-grade nickeliferous laterites. The surface morphology of the adsorbent was characterized by scanning electron microscopy. The adsorption experiment indicated a maximum nickel load capacity of about 0.45 mmol/g. Analysis of adsorption thermodynamic and kinetics revealed a spontaneous adsorption process driven by entropy increase, and limited by film diffusion. Semi-industrial scale column experiments revealed that the Ni^{2+} in the acidic leach liquor of low-grade nickeliferous laterites may be efficiently extracted by the iminodiacetic acid functionalized adsorbent, if the Fe^{3+} ions existing in the acidic leach liquor were previously reduced to be Fe^{2+} by sodium sulfite. This environmentally safe adsorbent may supplant the traditional solvent extraction process for low-grade nickeliferous laterites. *AIChE J,* 58: 3818–3824, 2012
Keywords: adsorbent, nickel, low grade, nickeliferous laterite, hydrometallurgical extraction

Introduction

Nickel is a strategic metal widely used for stainless steel,[1] electroplating,[2] nickel–metal hydride battery,[3] catalyst,[4–7] and so forth. Although 65% of nickel reserved in oxide ores, 70% of nickel products derived from sulfide ores.[8] Currently, hydrometallurgical process for low-grade nickeliferous laterites attract increasing attention, which involves ores leaching, nickel extraction from aqueous leach liquor, and electrowinning of nickel. Ammonia–ammonium carbonate leaching,[9] sulfation–roasting–leaching,[10] atmospheric acid leaching,[11] and high-pressure acid leaching[12,13] are often used for the leaching of nickeliferous laterites. In the nickel extraction step, carboxylic acid (such as Versatic 10)[14] and dithio-phosphinic acid-based extractant (such as Cyanex-301)[15,16] are commonly used for acidic leach liquor, whereas hydroxyoxime-based extractant (such as Lix 84)[17] is only used for ammoniacal leach liquor.

Because there are substantial amount of ferric ions in the acidic leach liquor, carboxylic acid and dithio-phosphinic acid-based extractant are unable to extract nickel unless the ferric ions were previously removed by chemical

Correspondence concerning this article should be addressed to X. Li at mzlixin@sina.cn, and D. Chen at genecarer@sina.com.

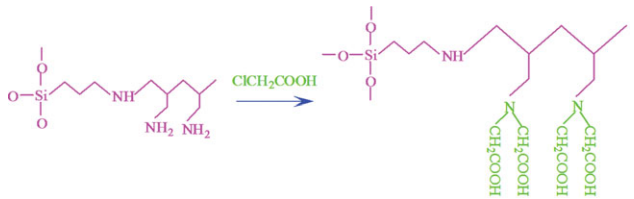

Scheme 1. Synthesis of SB-IDA adsorbent by grafting chloroacetic acid onto the SPC.

precipitation.[16] Furthermore, the organic extractant and solvent are typically toxic, flammable, and have adverse environmental impacts, it is essential to develop a more environmentally safe method for hydrometallurgical extraction of nickel.

An alternative to the solvent extraction processing of the acidic leach liquor is the use of polymer-based resins as an extraction medium. However, the elastic polymer-based resins is often subjected to alternate contraction–expansion during the adsorption–regeneration cycles, leading to short lifetimes and requisites of a dead volume in designing exchange column. Herein, we turned our attention to functionalized silica beads because the rigid nature of the silica matrices allows the materials to keep superior stability and durability even in frequent adsorption–regeneration cycles, which is particularly well-suited to packed column application. We were guided by the fact that ethylenediaminetetraacetic acid (EDTA) is a good chelating ligand for nickel. In this way, we designed and prepared silica-based iminodiacetic acid functionalized adsorbent (abbreviated as SB-IDA adsorbent, containing the functional group which is essentially a half EDTA molecule) for hydrometallurgical extraction of nickel.

In this article, nickel adsorption performances of SB-IDA adsorbent in different conditions were investigated and the adsorption conditions were optimized. Attempts are also made to evaluate its applicability in nickel hydrometallurgical extraction by continuous column adsorption–regeneration runs on a semi-industrial scale.

Materials and Methods

Materials

Raw silica gel was obtained from Qingdao Haiyang, China (particle size 150–500 μm, average pore diameter 15 nm, surface area 250 m^2/g). γ-Chloropropyl trimethoxysilane (CPTMOS) was purchased from Nanjing Yudeheng Fine Chemicals, China. Polyallylamine (PAA, MW 15,000, 15 wt % aqueous solution) was supplied by Nitto Boseki, Tokyo, Japan. Chloroacetic acid and solvents were provided by Jinan Jiahua Chemicals, China. Low-grade nickeliferous laterite ore is received from Indonesia. All chemicals were used as received except for the raw silica gel.

Preparation of SB-IDA adsorbent

Chloropropylated silica gel was first prepared by grafting CPTMOS onto raw silica gel and then reacted with PAA to get silica-polyallylamine composites (SPC), as described in the literature.[18] *N*-Alkylation between chlorine of chloroacetic acid and primary amino groups on SPC was then carried out to produce the designed SB-IDA adsorbent. A typical synthetic procedure was described as follows. Ten parts of chloroacetic acid, 10 parts of SPC, and 50 parts of water were placed into a reactor equipped with a stirrer to start the grafting reaction. The reaction was carried out at 70°C for 20 h to yield the SB-IDA adsorbent. The synthetic procedure of SB-IDA adsorbent was presented in Scheme 1.

Surface morphology of SB-IDA adsorbent

The surface morphology of SB-IDA adsorbent was determined by SEM. SEM was performed on a HITACHI S3500N microscope at 20 kV. For samples preparation, the dried adsorbent particles were fixed on a microscope slide and then were sprayed with a 3-nm thin gold layer.

Adsorption experiments

Batch adsorption tests were conducted in 250-mL glass flasks. To start the experiments, a desired amount of SB-IDA adsorbent particles were added to a 100 mL solution containing known metal ions. The flasks were placed in a incubator shaker and shaken under 200 rpm for 4 h at 298 K and specified pH to ensure equilibrium of the adsorption process. Column adsorption tests were performed on a glass column (10 mm diameter and 150 mm length) with a bed volume (BV) of 10 mL. A Master Flex L/S Model 77200-60 pump (Cole-Parmer Instrument Company) was used to ensure a constant flow rate. The concentration of all metal ions was measured by atomic adsorption spectroscope (Thermal) before and after adsorption.

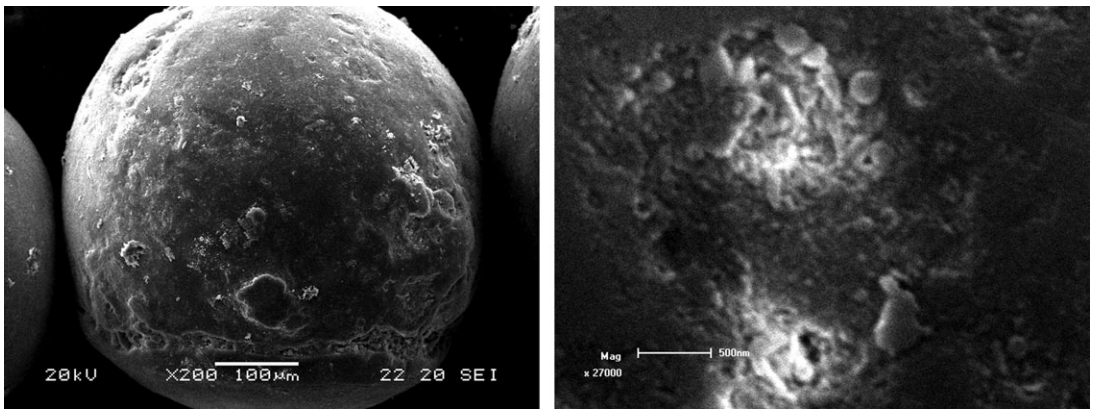

Figure 1. SEM images of SB-IDA adsorbent.

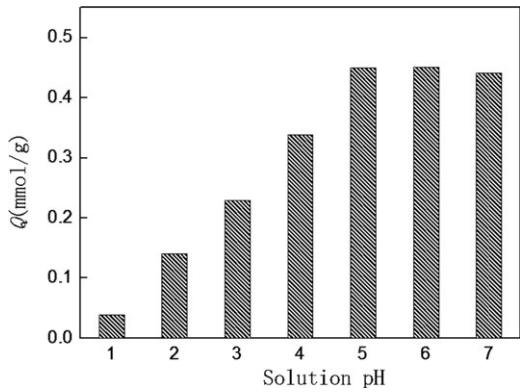

Figure 2. Effect of pH on Ni^{2+} adsorption at 298 K with an initial Ni^{2+} concentration of 1000 mg/L.

Results and Discussion

Surface morphology of SB-IDA adsorbent

The SEM images of the resultant SB-IDA adsorbent are shown in Figure 1, indicating a spherical shape of the adsorbent. The images also clearly reveal that the adsorbent particles have a rough surface with apparent micropores on it. The large surface area and abundant micropores should be favorable for the adsorption.

Effect of pH

Figure 2 depicts the effect of pH on Ni^{2+} batch adsorption capacity in aqueous solution at 298 K with an initial Ni^{2+} concentration of 1000 mg/L. In the pH range of 1.0–5.0, an increase in pH resulted in a rise in Ni^{2+} adsorption capacity. A maximum adsorption capacity of 0.45 mmol/g was observed at pH of 5.0. As the pH increased further, the Ni^{2+} adsorption capacity began to drop. The pH-dependence of Ni^{2+} adsorption may be interpreted as follows. Iminodiacetic acid groups on the adsorbent will deprotonate when increasing the solution pH which is favorable for chelating Ni^{2+} and, thus, for adsorption. However, at a pH above 5.0 precipitation of $Ni(OH)_2$ may occur in the solution or within the adsorbent particles according to its solubility product. Therefore, a pH of about 5.0 is preferred for adsorption process.

Adsorption isotherms and thermodynamics

Figure 3 shows the equilibrium adsorption isotherms of SB-IDA adsorbent at different temperatures. The adsorption capacity increased as the adsorption temperatures increased. Adsorption isotherms of Ni^{2+} onto SB-IDA adsorbent at different temperatures are represented by the Freundlich equation.

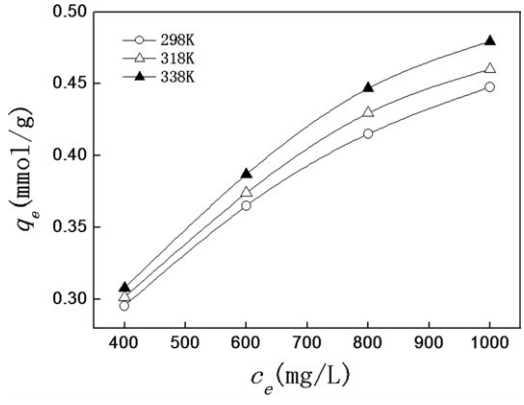

Figure 3. Equilibrium adsorption isotherms of Ni^{2+} onto the SB-IDA adsorbent at different temperatures.

Table 1. Freundlich Isotherm Parameters of Ni^{2+} onto SB-IDA Adsorbent at Different Temperatures

T (K)	n	R^2
298	2.3267	0.9933
318	2.2676	0.9915
338	2.1636	0.9903

$$\ln q_e = \ln k_F + \frac{1}{n}\ln c_e \quad (1)$$

where q_e is the equilibrium adsorption capacity, c_e represents the solute concentration at equilibrium, k_F and n are the Freundlich constants to be determined. The Freundlich model was found to represent all the Ni^{2+} adsorption isotherms reasonably, as indicated by its high relative coefficient values (larger than 0.99, as listed in Table 1).

If liquid-phase adsorption follows the Freundlich model, thermodynamic parameters for the adsorption process such as free energy change (ΔG), enthalpy change (ΔH), and entropy change (ΔS) can be calculated with the following equations[19,20]

$$\Delta G = -nRT \quad (2)$$

$$\ln c_e = -\ln k_0 + \frac{\Delta H}{RT} \quad (3)$$

$$\Delta G = \Delta H - T\Delta S \quad (4)$$

where n is the Freundlich constant, R is the gas constant (8.314 kJ/mol•K), T is the absolute temperature (K), and k_0 is a constant. The free energy change is calculated by Eq. 2 and the enthalpy change is deduced from the slope of van't Hoff plots ($\ln c_e$ vs. $1/T$). Then, the entropic contribution can be subsequently determined according to Eq. 4. Figure 4 shows the van't Hoff plots with calculated thermodynamic parameters. The negative ΔG (−5.76 KJ/mol when T is 298 K) value indicates feasibility and spontaneous nature of adsorption process. Furthermore, the positive values of ΔH (1.62 KJ/mol) and ΔS (26.77 J/mol·K) reveal an endothermic process driven by entropy increase. A reasonable explanation for these thermodynamic parameters may be given as follows. As nickel ions generally exist in $Ni(H_2O)_6^{2+}$ in the aqueous solution, the

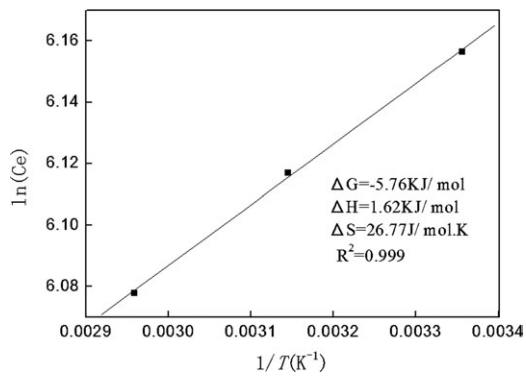

Figure 4. Van't Hoff plots ($\ln C_e$ vs. $1/T$) for the adsorption.

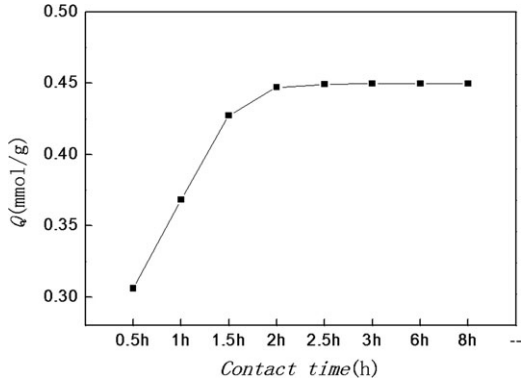

Figure 5. Adsorption kinetic curve of SB-IDA adsorbent at 298 K and pH 5.0 with an initial Ni concentration of 1000 mg/L.

adsorption process means the dissociation of hydrated nickel ions followed by the chelating of the bare nickel ions onto the SB-IDA adsorbent matrix. It can be believed that during the adsorption process, the water molecules of $Ni(H_2O)_6^{2+}$ were dissociated to be individual and more disordered ones leading increased randomness.

Adsorption and desorption kinetics

Figure 5 presents the plot of Ni^{2+} batch adsorption capacity vs. contact time for SB-IDA adsorbent with an initial Ni concentration of 1000 mg/L. An equilibrium load capacity of 0.45 mmol/g was observed at about 2 h, indicating a sufficiently rapid adsorption kinetics.

In general, the adsorption process can be interpreted by a series of steps: (a) mass transfer of solute from the liquid to the particle surface across the boundary layer, (b) diffusion of solute within the pores and deposition on the surface of the particles, and (c) chemical reaction of the solute with the functional groups attached to the matrix.[21,22] One of the steps usually exhibits much greater resistance than the other two, and this step is considered as the rate-limiting step of the adsorption process. To determine which step (film diffusion, intraparticle diffusion, or chemical reaction) played a dominant role and to obtain the corresponding rate constants, the kinetic data presented in Figure 5 were further processed. The following three models, each assuming a different rate-limiting step in the adsorption process, were used to fit the experimental data:[23]

Film diffusion model

$$\ln(1-F) = -k_f t \tag{5}$$

Intraparticle diffusion model

$$q_t = k_p t^{1/2} \tag{6}$$

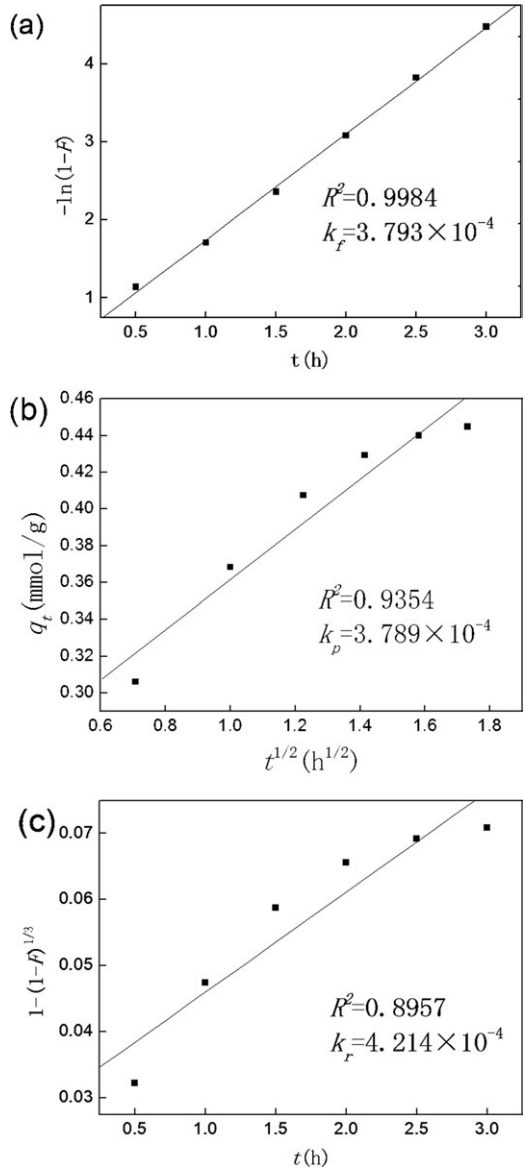

Figure 6. Plots of adsorption kinetic curve at 298 K fitting with (a) film diffusion model, (b) intraparticle diffusion model, and (c) chemical reaction model.

Chemical reaction model

$$1-(1-F)^{1/3} = k_r t \tag{7}$$

where k_f, k_p, and k_r are the rate constants for film diffusion, intraparticle diffusion, and chemical reaction, respectively; and F (q_t/q_e) is the fractional attainment of the equilibrium. The fitting results with Eqs. 5–7 are presented in Figure 6.

Table 2. A Comparison of the Physical Characteristics and Nickel Adsorption Capacities of SB-IDA Adsorbent and Amberlite IRC-718

				Adsorption Capacities (mmol/g)*	
Entry	Appearance	Particle Size (μm)	Density (g/mL)	Batch Test	Flow Test†
SB-IDA	Light yellow particles	150–500	0.50	0.45	0.43
IRC-718	Opaque beige beads	300–1180‡	0.68‡	0.73	0.38

*Determined experimentally at 298 K.
†Determined at a flow rate of 6 BV/h.
‡Data from manufacturer.

Table 3. Adsorption Capacity of Ni^{2+} in the Perturbance of Different Perturbing Ions at 298 K and pH 5.0, with an Initial Concentration of 1000 mg/L for Nickel and All Perturbing Ions

Perturbing Ions	WPI	Cu^{2+}	Zn^{2+}	Co^{2+}	Mn^{2+}	Fe^{2+}	Ca^{2+}	Mg^{2+}
Q (mmol/g)	0.45	0.25	0.38	0.43	0.43	0.43	0.44	0.45

WPI: without perturbing ions

Clearly, the film diffusion model leads to much better regression coefficients (0.9984) than the other two models, indicating that the adsorption process is limited by film diffusion.

A comparison of adsorption capacities between SB-IDA adsorbent and Amberlite IRC-718

As hydrometallurgical extraction of nickel is operated in column, the adsorption performance of the adsorption materials under dynamic (flow) condition should be more important than under static (batch) condition. Herein, additional flow studies were performed to determine the nickel capacity of SB-IDA adsorbent in repeated adsorption/desorption cycles at room-temperature. For comparison, experiments were also conducted on a typical iminodiacetic acid functionalized cross-linked polystyrene resin, Amberlite IRC-718, which is commercially available from Rohm and Haas. The physical characteristics and nickel adsorption capacities of SB-IDA adsorbent and Amberlite IRC-718 were shown in Table 2. IRC-718 exhibits a higher nickel adsorption capacity in batch tests, which may be due to its more available adsorption sites. SB-IDA adsorbent, however, has a greater capacity in flow tests. This result is not surprising and may suggest that, in flow tests, the aqueous nickel ion solution is forced through adsorption materials and the nickel ions take longer to come into contact with the chelating groups on the hydrophobic polystyrene resin matrix, compared with the hydrophilic SB-IDA matrix, and thus, less of the nickel ions can effectively reach the available binding sites of IRC-718 than those of SB-IDA during flow tests.

Nickel adsorption performance in the presence of perturbing ions

It is important to know the adsorption performance for Ni^{2+} in the presence of naturally occurring cations such as Cu^{2+}, Zn^{2+}, Co^{2+}, Mn^{2+}, Ca^{2+}, Mg^{2+}, and iron. It is known that iron generally exists in ferric ion and it will involve two adverse factors: (a) strong adsorption of ferric ions onto the adsorbent. The electrostatic attraction between $-CH_2COO^-$ and Fe^{3+} is stronger than that between $-CH_2COO^-$ and divalent cations, so that the SB-IDA adsorbent will prefer to adsorb Fe^{3+} and, thus, lose the ability to adsorb Ni^{2+}. (b) Precipitation of $Fe(OH)_3$ within the SB-IDA adsorbent particles will easily occur due to the low solubility products of $Fe(OH)_3$, which leads to a foul adsorbent. As the two adverse factors cause deterioration in adsorption performance of Ni^{2+}, sodium sulfite was used to reduce ferric ions into ferrous ions before adsorption so as to avoid the adverse influence of ferric ions.

Herein, the influence of Cu^{2+}, Zn^{2+}, Co^{2+}, Mn^{2+}, Ca^{2+}, Mg^{2+}, and Fe^{2+} on batch adsorption capacity of Ni^{2+} was estimated, respectively, the initial concentrations of nickel and all the perturbing ions were 1000 mg/L. The results shown in Table 3 revealed that the influence of perturbing ions on nickel adsorption capacity followed the order: $Cu^{2+} > Zn^{2+} > Co^{2+} > Mn^{2+} > Fe^{2+} > Ca^{2+} > Mg^{2+}$. It was also seen that ferrous ions has a negligible influence on the adsorption capacity of Ni^{2+}.

Figure 7. A set of three packed columns for Ni hydrometallurgical extraction of low-grade nickeliferous laterites.

Semi-industrial scale column experiments in Ni hydrometallurgical extraction of low-grade nickeliferous laterites

The leaching of low-grade nickeliferous laterite was achieved with sulfuric acid at atmospheric pressure. Then, sodium sulfite was added to the acidic leach liquor to reduce ferric ions into ferrous ions. After careful filtration, the pH value of the acidic leach liquor was adjusted to 5.0 for best adsorption of Ni^{2+}. The semi-industrial scale column experiments of the acidic leach liquor were conducted as follows: a set of three packed columns provide a continuous adsorption–regeneration operation (see, Figure 7). Two of the columns are connected in series, and the third column serves as a spare. The hydrometallurgical extraction of nickel takes place in the two connected columns, whereas the other one is being purged/regenerated or otherwise for repair or routine maintenance. All treatment streams are introduced in a counterflow way (i.e., the solution was continuously pumped in from the bottom of column and discharged after treatment from the top of column), so that the streams can be in adequate and intimate contact with SB-IDA adsorbent. In this operation, each column is packed with 100 L SB-IDA adsorbent. The operating flow rate was optimized to be 6 BV/h.

The composition of acidic leach liquor of Indonesia low-grade nickeliferous laterite is shown in Table 4 (feed solution). Figure 8 revealed that Ni^{2+} can be efficiently extracted within about 20 BV per run before a significant breakthrough occurred (it is determined that the concentration of the specified ions remaining in effluent after column adsorption exceeds 1.0 mg/L), whereas Fe^{2+}, Mn^{2+}, and Mg^{2+} were almost not adsorbed. On completion of the fixed-bed

Table 4. Concentration Comparisons of Each Metal Ion in Feed and Strip Solution During an Adsorption–Regeneration Run

Solution	Concentration of Metal Ions (mg/ L)								
	Ni^{2+}	Cu^{2+}	Fe^{2+}	Co^{2+}	Mn^{2+}	Pb^{2+}	Zn^{2+}	Mg^{2+}	Ca^{2+}
Feed	687.2	5.37	16,448	27.24	223.91	0.012	4.14	251.94	1.30
Strip	25,479	20.93	66.93	65.09	7.08	0.013	0.84	9.26	0.23

adsorption, the exhausted resin was regenerated first rinsing with 5 BV H_2SO_4 solution of pH 5.0 for a chase of the residual background ions, followed by stripping the bound Ni^{2+} with H_2SO_4 solution of 100 g/L, and then, washing to pH 5.0 with water for reuse. It is also seen from Table 4 that Ni^{2+} was concentrated to a high level of 25,479 mg/L in strip solution from 687.2 mg/L in feed solution, whereas Fe^{2+} and other metal ions were limited in a very low concentration. The results of more than continuous 500 adsorption–regeneration runs indicated that the adsorbent presented constantly adsorption capacity for Ni^{2+}, and more than 98% of Ni^{2+} in the feed solution can be extracted to be high purity Ni^{2+} solutions.

It was reported[24] that high-quality crystalline nickel was deposited in cathode when the electrolyte for electrowinning containing 60 g/L of Ni^{2+}, 100 mg/L of Cu^{2+}, 500 mg/L of Fe^{3+}, and 500 mg/L of Co^{2+} with operation temperature of 30°C and current density of 400 A/m^2, and the current efficiency reached as high as 97%. Therefore, if the strip solution from the semi-industrial scale column experiments was concentrated to a half volume, it would be suitable for the final nickel electrowinning. The result suggests a potential industrial application of the adsorption for nickel recovery from low-grade nickeliferous laterite.

Conclusions

It is a challenging task to develop an environmental-friendly process for nickel extraction from low-grade nickeliferous laterites in the presence of substantial amount of iron. To deal with the task, SB-IDA was fabricated and the adsorption conditions for nickel extraction were optimized. Adsorption experiments showed that SB-IDA adsorbent reached a maximum adsorption capacity of 0.45 mmol/g for Ni^{2+} at pH 5.0. Adsorption thermodynamic and kinetics analysis revealed a spontaneous adsorption process driven by entropy increase, and limited by film diffusion.

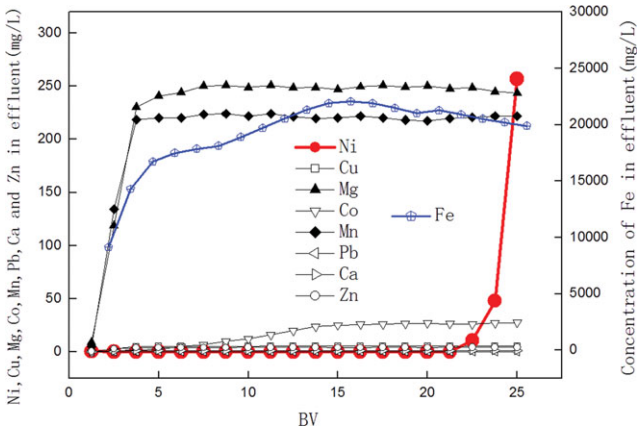

Figure 8. Adsorption breakthrough curves of nickel and other metal ions of the acidic leach liquor under a continuous column operation.

Then, SB-IDA adsorbent was used to process the acidic leach liquor of low-grade nickeliferous laterites. As Fe^{3+} will foul the SB-IDA adsorbent, whereas Fe^{2+} has a negligible influence on the adsorption capacity of Ni^{2+}, the Fe^{3+} ions existing in the acidic leach liquor were previously reduced to be Fe^{2+} by sodium sulfite. The semi-industrial scale column experiments for the acidic leach liquor indicated that more than 98% Ni^{2+} in leach liquor can be extracted to be high purity Ni^{2+} solutions only containing slight amount of iron and other metal ions. The result enables an industrial application for hydrometallurgical nickel extraction from low-grade nickeliferous laterites.

Literature Cited

1. Bertolini L, Gastaldi M. Corrosion resistance of low-nickel duplex stainless steel rebars. *Mater Corros*. 2011;62:120–129.
2. Schlesinger M, Paunovic M, Di Bari GA. *Electrodeposition of nickel*. In: Schlesinger M, Paunovic M, editors. *Modern Electroplating*, 5th ed. New York: Wiley, 2011:79–114.
3. Cheng F, Liang J, Tao Z, Chen J. Functional materials for rechargeable batteries. *Adv Mater*. 2011;23:1695–1715.
4. Zhong Z, Xing W, Jin W, Xu N. Adhesion of nanosized nickel catalysts in the nanocatalysis/UF system. *AIChE J*. 2007;53:1204–1210.
5. Peng Y, Dong M, Meng X, Zong B, Zhang J. Light FCC gasoline olefin oligomerization over a magnetic $NiSO_4/\gamma$-Al_2O_3 catalyst in a magnetically stabilized bed. *AIChE J*. 2009;55:717–725.
6. Liu J, Harris AT. Synthesis of multiwalled carbon nanotubes on Al_2O_3 supported Ni catalysts in a fluidized-bed. *AIChE J*. 2010;56:102–113.
7. Zhang C, Li S, Li M, Wang S, Ma X, Gong J. Enhanced oxygen mobility and reactivity for ethanol steam reforming. *AIChE J*. 2012;58:516–525.
8. Anthony MT, Flett DS. Nickel processing technology: a review. *Miner Ind Int*. 1997;1:26–42.
9. Zhai Y, Mu W, Liu Y. A green process for recovering nickel from nickeliferous laterite ores. *Trans Nonferrous Metals Soc China*. 2010;20:65–70.
10. Guo X, Li D, Park KH. Leaching behavior of metals from a limonitic nickel laterite using a sulfation-roasting-leaching process. *Hydrometallurgy*. 2009;99:144–150.
11. McDonald RG, Whittington BI. Atmospheric acid leaching of nickel laterites review. Part I: Sulfuric acid technologies. *Hydrometallurgy*. 2008;91:35–55.
12. Georgiou D, Papangelakis VG. Sulfuric acid pressure leaching of a limonitic laterite: chemistry and kinetics *Hydrometallurgy*. 1998;49:23–46.
13. Rubisov DH, Papangelakis VG. Sulfuric acid pressure leaching of laterites: a comprehensive model of a continuous autoclave. *Hydrometallurgy*. 2000;58:89–101.
14. Tsakiridis PE, Agatzini SL. Process for the recovery of cobalt and nickel in the presence of magnesium and calcium from sulphate solutions by Versatic 10 and Cyanex 272. *Miner Eng*. 2004;17:535–543.
15. Jakovljevic B, Bourget C, Nucciarone D. Cyanex 301 binary extractant systems in cobalt/nickel recovery from acidic chloride solutions. *Hydrometallurgy*. 2011;109:187–258.
16. Tsakiridis PE, Agatzini SL. Simultaneous solvent extraction of cobalt and nickel in the presence of manganese and magnesium from sulfate solutions by Cyanex 301. *Hydrometallurgy*. 2004; 72:269–278.
17. Parija C, Bhaskara Sarma PVR. Separation of nickel and copper from ammoniacal solutions through co-extraction and selective stripping using LIX84 as the extractant. *Hydrometallurgy*. 2000;54: 195–204.
18. Hughes MA, Nielsen D, Rosenberg E. Structural investigations of silica polyamine composites: surface coverage, metal ion coordination, and ligand modification. *Ind Eng Chem Res*. 2006;45:6538–6547.

19. Pan B, Zhang Q, Meng F, Li T, Zhang X, Zhang W, Chen J. Sorption enhancement of aromatic sulfonates onto an aminated hypercrosslinked polymer. *Environ Sci Technol*. 2005;39:3308–3313.
20. Gupta VK, Ali I, Saini VK. Removal of chlorophenols from wastewater using red mud: an aluminum industry waste. *Environ Sci Technol*. 2004;38:4012–4018.
21. Dutta M, Baruah R, Dutta NN. Adsorption of 6-aminopenicillanic acid on activated carbon. *Sep Sci Technol*. 1997;12:99–108.
22. Li X, Liu R, Wu S, Liu J, Cai, S, Chen D. Efficient removal of boron acid by *N*-methyl-D-glucamine functionalized silica-polyallylamine composites and its adsorption mechanism. *J Colloid Interf Sci*. 2011;361:232–237.
23. Onal Y, Akmil-Basar C, Sarici-Ozdemir C. Investigation kinetics mechanisms of adsorption malachite green onto activated carbon. *J Hazard Mater*. 2007;146:194–203.
24. Gogia SK, Das SC. The effect of Co^{2+}, Cu^{2+}, Fe^{2+} and Fe^{3+} during electrowinning of nickel. *J Appl Electrochem*. 1990;24:64–72.

Manuscript received Dec. 2, 2011, and revision received Jan. 19, 2012.